Pickup Particle Acceleration at Comets, Moons and Magnetospheres

Andrew J. Coates

Mullard Space Science Laboratory, University College London, Holmbury St Mary, Dorking RH5 6NT

a.coates@ucl.ac.uk

Abstract. Ionisation of neutrals plays a key role in the plasma interactions of comets and moons, and in magnetospheres. Following ionisation, ions and electrons are 'picked up' in the plasma flow, initially accelerating along the electric field and then gyrating around the magnetic field. For an ion with mass m (amu) this leads to an acceleration of up to 4m times the energy of the flowing plasma. Further scattering in pitch angle and energy may increase the acceleration further. Here, we illustrate the process at work with relevant plasma measurements from comets including Rosetta's comet 67P, from Titan and near Enceladus and Rhea.

1. Introduction

The pickup process begins when neutral particles from a comet or atmosphere are ionized by sunlight, electron impact or charge exchange. Neutral particles may come from a comet's coma, an atmosphere or interplanetary neutral particles. A summary of loss rates at solar system objects was given by Coates [1, see Figure 1].

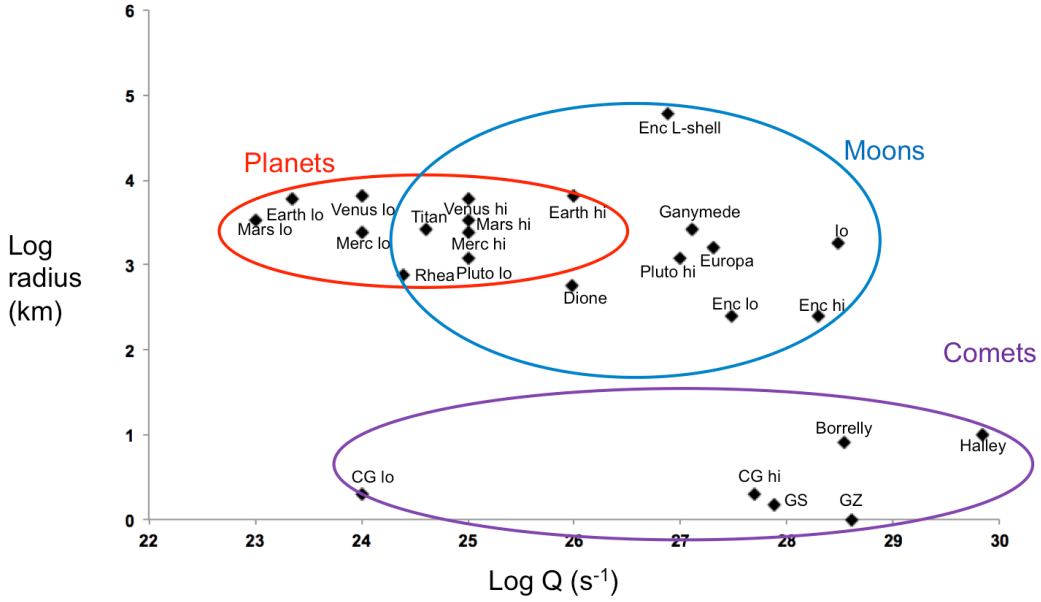

Figure 1 - Summary of neutral production rates (Q) for solar system objects compared to body radius (see [1] for details)

A summary of the pickup process is illustrated in Figure 2. In this paper, we will discuss the stages in the ion pickup process and illustrate each stage with examples from spacecraft data. We will also discuss the acceleration of particles as a result of pickup and from processes beyond pickup.

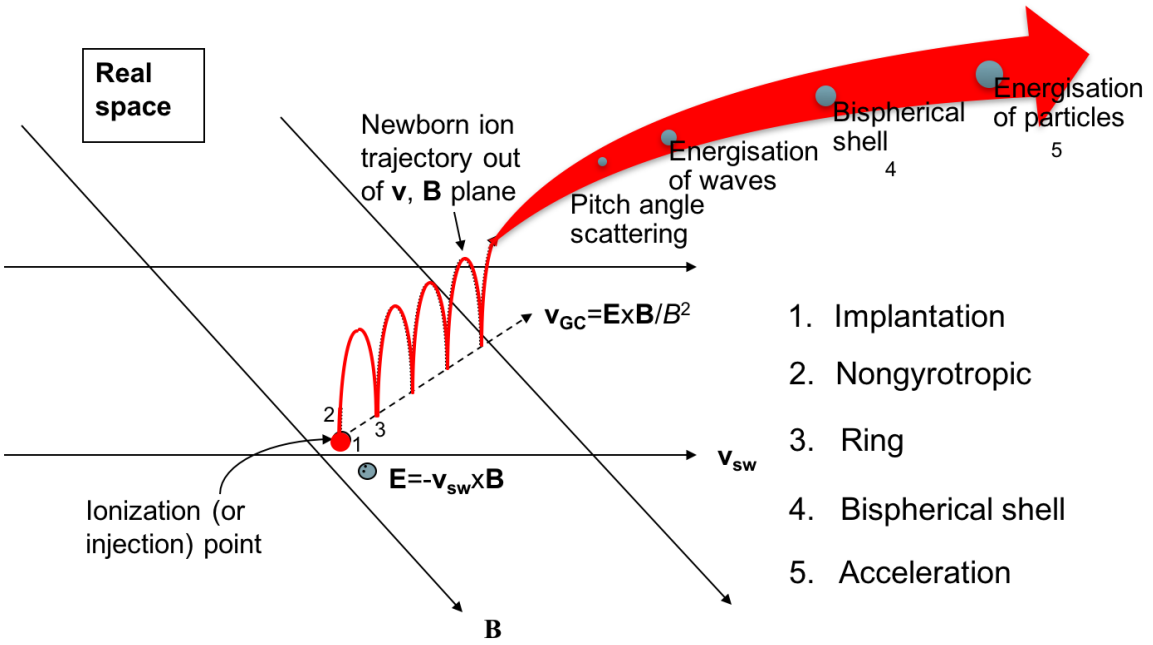

Figure 2 - Stages in the ion pickup process

2. Summary of stages in the ion pickup process

Following ionization, the particle is 'implanted' (Stage 1 in Table 1), and is then subject to the electric (**E**) and magnetic (**B**) fields in the collisionless flowing plasma. The particle is initially accelerated along the electric field, and in the ideal MHD approximation **E** = - **v** x **B**. The particle then gyrates around the magnetic field, with its initial motion as seen in **E** x **B** drift.

If there is a gradient in neutral particle density which is significant with respect to the particle's gyroradius, or at distances within ~2 gyroradii of the injection point, a 'non-gyrotropic' distribution of particles may occur (Stage 2), and has been observed at weak comets [2,3] and moons [4,5].

Table 1 – Stages in the ion pickup process, with indication of where each stage has been seen in spacecraft plasma observations. C=Comets, Ma=Mars, Mo=Moon, Msph=magnetospheres, V=Venus, Io=Io, E=Enceladus, T=Titan, R=Rhea, D=Dione, I=Interstellar

Stage in process	**Timescale**	**Seen at**
1. Implantation	<< gyroperiod (f_{ci})	C
2. Nongyrotropic ring	<gyroperiod	C, R, D, T
3. Ring	~gyroperiod	C, Ma, Mo, Msph, V, Io, E, T, I, R, D
4. (Bispherical) shell	~10 gyroperiods	C, Io?, E?, I?
5. Acceleration, shell filling	~100 gyroperiods	C
6. Maxwellian	?	?

Following this, and after at least a full gyration, the particle follows a cycloid in real space, corresponding to a ring in velocity space (Stage 3). The ring is unstable to plasma waves and instabilities, and the particle distribution becomes scattered in pitch angle, with energy being given to plasma waves.

The consequence of this conservation of energy, with energy being given by the particles to the waves, is a bispherical shell particle distribution (Stage 4) [6, and references therein]. Further wave-particle interactions and Fermi type II acceleration provides further energization, and slowing, of the particles – 'energy diffusion' (Stage 5). This process leads to both acceleration and shell filling, and finally (Stage 6) the particle distribution tends towards a Maxwellian.

Table 1 summarises the stages in the ion pickup process. We now consider the observations associated with each of the stages of pickup.

3. Stage 1 – Implanted ions

Newly implanted ions (or fresh pickup ions) have been seen in several cometary environments, but most recently by the Rosetta spacecraft at comet 67P [3,7]. In Figure 3 we show data from the Rosetta Ion and Electron Spectrometer instrument plotted over the whole Rosetta mission since orbit insertion in August 2014 to September 2016. The implanted ions are seen well below the energy of the solar wind in the second panel (ions). Although there are intervals where acceleration from the initial pickup energy is seen (Stage 2), many intervals particularly at large heliocentric distance (beginning and end of the plot) are characterized by low energy (<10eV) ions [3,7].

Note that in the case of Rosetta the spacecraft speed is very low (~cm s^{-1}) with respect to the comet. The initial, lowest energy at which Rosetta measures the pickup ions is dominated by the spacecraft potential [3]. During most of the interval shown the dominant plasma density is ionospheric and thus the spacecraft potential is a little negative, increasing their initial energy which is zero in the frame of the neutral particles. It is interesting that towards the beginning and end of the plot, the solar wind penetrates to Rosetta's position near to the cometary nucleus. There is therefore an electric field which can be seen accelerating the particles at times up to ~20-30 eV at heliocentric distances >~2.5 AU and frequently to 50-1000 eV for heliocentric distances <~2.5 AU (Stage 2).

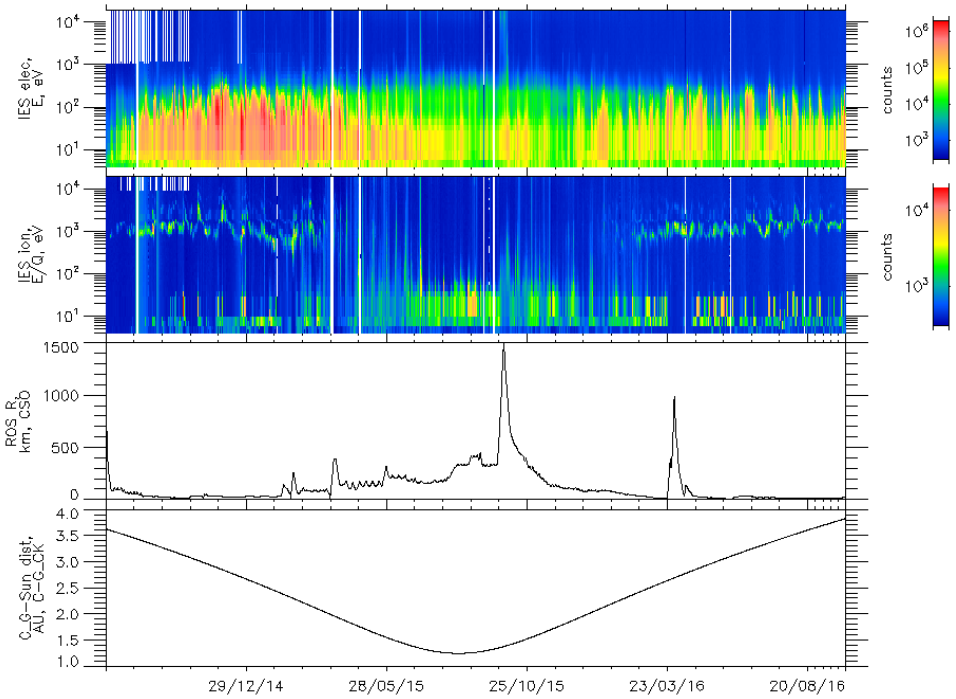

Figure 3 - RPC IES data from comet 67P. The top panel shows electrons, second panel shows ions, the third panel shows the Rosetta-comet distance and the 4th panel shows the comet-Sun distance.

4. Stage 2 – Nongyrotropic rings

The next stage of the pickup process beyond low energy (in the neutrals' frame) is the acceleration of the pickup ions along the electric field and the beginnings of gyration around the magnetic field. In the Rosetta data we already saw examples of such acceleration in Section 3. Further examples, and a comparison with pickup ions observed in the AMPTE neutral lithium and barium releases in 1984-5, were shown in [8]. The ion distributions observed in both the AMPTE and Rosetta data show a characteristic increasing energy due to following pickup ions around the early phase of the pickup ion trajectory. These constitute nongyrotropic distributions in velocity space [8].

Another way of producing a nongyrotropic distribution is at a more active, but still weak, comet such as Grigg-Skjellerup [2]. In this case, the ion production rate which decreases with distance from a cometary nucleus, varies between the cusps of the cycloid trajectory of pickup ions enough that the density changes with gyration angle. This was observed by Giotto at comet Grigg-Skjellerup [3] and led to the production of different instabilities [9,10].

An extreme version of this is the observation of pickup ions from moons with weak exospheres where pickup ions are observed originating from near the moon's surface. This was observed by the Cassini spacecraft at Rhea [4] and Dione [5], and has been seen as one of the pickup populations near Earth's moon [11].

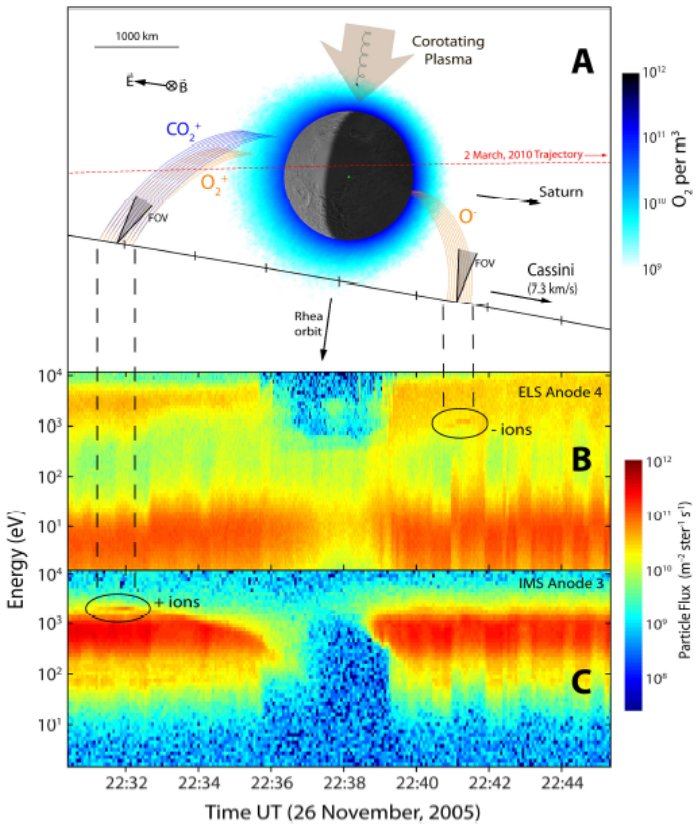

Figure 4 - Cassini CAPS observations of pickup ions near Rhea. Positive and negative pickup ions are seen, locating their source in a weak near-surface atmosphere (from [4])

Figure 4 shows observations by the CAPS instrument near to Saturn's moon Rhea. The bottom panel shows positive ions, with a narrow (in energy) pickup ion population seen before closest approach to the moon, likely O^+, superimposed on the corotating magnetospheric ion population before the spacecraft enters the plasma wake of Rhea. The middle panel shows data from the CAPS electron spectrometer, including cold magnetospheric electrons (<~20 eV), injection related hot

electrons (~1-5 keV) and the Rhea plasma wake. After closest approach, a narrow population of negative pickup ions is seen, likely O^-. Trajectory modelling of the early trajectory pickup ions locates the source near the moon and this, together with INMS measurements of neutral O_2 and CO_2, represents the discovery of Rhea's weak atmosphere. This is due to sputtering by magnetospheric ions, and is also present at Dione [5], and at Europa and Ganymede in the Jupiter system the target of the JUICE and Europa Clipper missions. For our purposes here, these are remarkable observations of Stage 2 positive and negative pickup ions.

Recently, pickup ion observations at Titan were re-examined [12,13] and the dominant direction of the early trajectory was confirmed to be along the E direction [13]. In addition, the loss rate due to pickup was found to be ~3.3×10^{23} s^{-1} [13], compared to about an order of magnitude higher rate from the ionosphere [14].

5. Stages 3,4 and 5 – Rings, bispherical shells, acceleration

The classical pickup process produces, after the early stages described above, rings in velocity space, bispherical shells and particle acceleration. After executing a complete cusp to cusp gyration in real space (early gyrations in Figure 2) the particle distribution function becomes a ring. These distribution functions are observed at comets (e.g. [1] and references therein) and are unstable to waves, which produce pitch angle scattering.

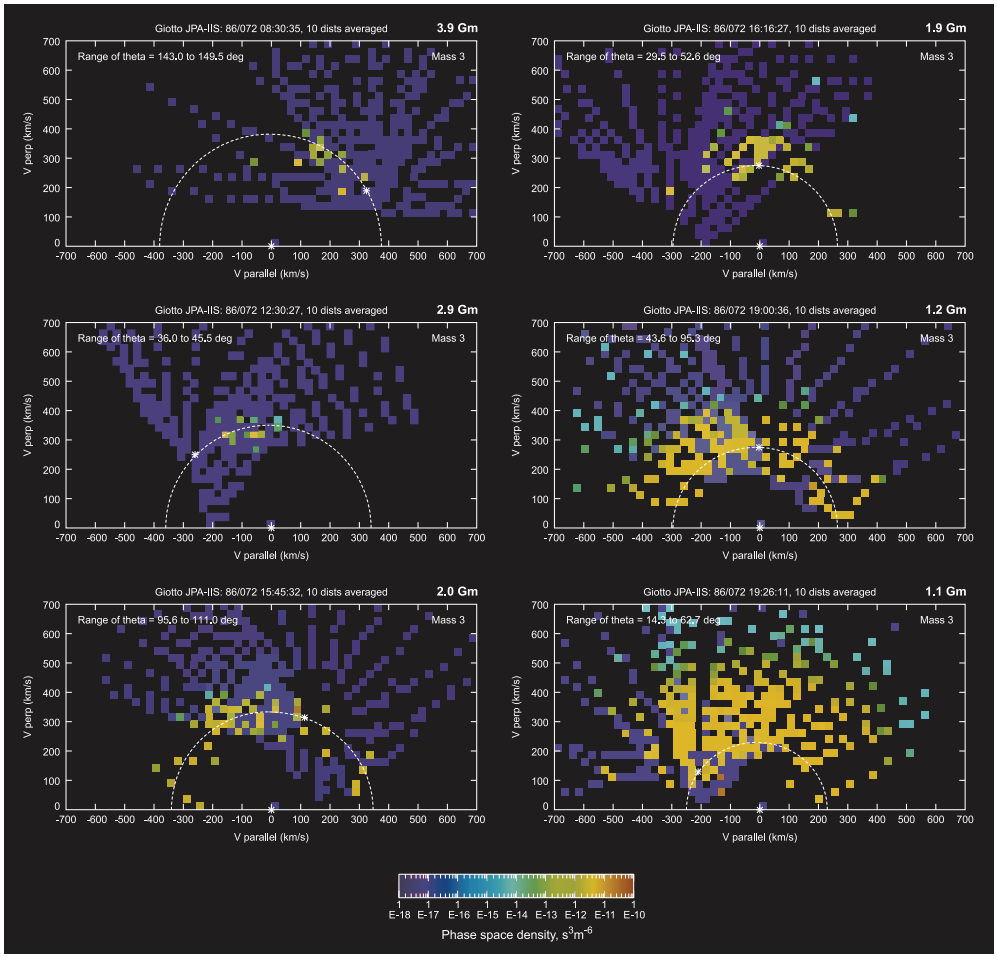

Figure 5 - Pickup water group ion distribution functions observed at comet Halley. The distribution follows the evolution from rings (upper left panels 1,2) to (bispherical) shell (panels 3,4) and shows particle acceleration upstream (panel 5) and downstream (panel 6) of the comet's bow shock (from [1], adapted from [15])

The maximum velocity of the ring with respect to the injection point (frame of the neutral particles) is $2|v|\sin\theta_{vB}$, where θ_{vB} is the angle between **v** and **B** and m is the ion mass in amu. Thus, the maximum energy of the ring is $2mv^2\sin^2\theta_{vB}$. This corresponds to $4mE_{sw}\sin^2\theta_{vB}$, where E_{sw} is the energy of the flowing plasma, for example the solar wind (see [1]).

Similarly, the maximum velocity of the bispherical shell is $2|v|$, thus the maximum energy is $4mE_{sw}$.

At the Moon, reflection of a fraction of neutral particles [11] gives additional acceleration and means that the maximum velocity of a bispherical shell is $3|v|$ in the lunar exosphere frame, and the maximum energy is $9mE_{sw}$ [11,1].

Stages 3,4 and 5 of the pickup process are well illustrated in Giotto data from the active comet Halley [15,16]; see Figure 5 (from [1]. In these plots the data have been transformed from the measured energy and angle dependent spectra in the spacecraft frame, to a magnetic field aligned solar wind frame [15], and arranged as $V_{\perp}$-$V_{\parallel}$ water group ion distributions. In this format, a ring distribution would appear at the point marked * on each plot, which denotes the injection point on the semicircle (representing the local solar wind velocity).

The first two panels are relatively narrow indicating limited scattering from the initial ring (*) around the semicircle, while the third and fourth panels show significant pitch angle scattering (almost around the entire semicircle). The bulk parameters of these populations (not shown) are consistent with bispherical shells centred on upstream and downstream propagating Alfven waves [16].

The fifth and sixth panels are samples immediately upstream and downstream of the cometary bow shock, and show significant acceleration beyond local pickup velocities. Although some of the pickup ions in these two panels are transported from upstream, the last panel in particular shows evidence of particle acceleration well beyond pickup. This is likely due second order Fermi processes with acceleration from the bispherical shell (stage 5) and first order Fermi acceleration associeated with approaching scattering centres near the bow shock [19,15]. The further accelerated ions are also seen in energetic particle detectors [20,21,22]. Pickup protons show somewhat similar behaviour [23].

Developed ring distributions are also seen in planetary magnetospheres. For example, in Saturn's magnetosphere near the orbit of Enceladus, the neutral particle density is about 2 orders of magnitude greater than the plasma density. Ring distributions of water group ions resulting from ionization of the neutrals were clearly seen there in the Cassini CAPS data [24]. The ions had ~90° pitch angle, consistent with the observation of early pickup ion rings in an almost dipolar magnetic field at ~4 Saturn radii.

6. Pickup ions dominate the comet-SW interaction

Here, we briefly summarise the solar wind-comet interaction and the relevant pickup ion processes. At weak comets, early phase implanted ions are important (Stage 1, section 3 above – see [25,8,3,7]). The mass loading associated with these slows the plasma enough that eventually a bow shock forms. Pickup ions play a key role at the bow shock [26,27,28].

The observed pickup water group ion distribution functions include Stage 1 implanted ions (Section 3), Stage 2 nongyrotropic rings [2], Stage 3 rings [15,23], and Stage 4 bispherical shells [16].

Acceleration beyond pickup (Stage 5) was also seen at comets Giacobini-Zinner [21,22], Halley [29,20,15,16] and at comet Grigg-Skjellerup [30,2,31,32].

7. Summary and conclusions

Plasma and magnetic field measurements are a sensitive indicator of cometary, moon and planetary activity in terms of neutral particle production rate, over many orders of magnitude of activity [1, see Figure 1]. Pickup ions result from the ionization of neutral particles in all these environments.

The ion pickup process includes different stages at weak, medium and strong comets, and we have summarized these in this paper (see Table 1 and sections 3-5). The different stages are clearly seen with Rosetta, Giotto and the other cometary missions.

The pickup process is also seen at moons (e.g., Rhea, Dione, Titan and Earth's moon). It is also seen in magnetospheres particularly where neutral particles dominate (e.g., Saturn's magnetosphere).

There is a clear need for particle and field measurements for activity detection at both weak and strong sources of neutral particles for future missions where activity and neutral particle production is important. One example of this is main belt comets [33,34].

Acknowledgments

We thank the organisers for the opportunity of giving this talk, and the STFC Consolidated Grant to UCL-MSSL for funding. I would also like to acknowledge the Giotto JPA, Cassini CAPS and Rosetta RPC teams for excellent collaboration for over 3 decades, and nearly 8 orders of magnitude in gas production rate. We thank Jim Burch and the RPC team for use of the data in Figure 3.

References

[1] Coates A J 2016 Plasma Measurements at Non-Magnetic Solar System Bodies *Magnetosphere-Ionosphere Coupling in the Solar System*, AGU Geophysical Monograph 222, ed C R Chappell, R W Schunk, P M Banks, J L Burch, and R M Thorne (Hoboken: Wiley) Chapter 21 pp259-276

[2] Coates A J, Johnstone A D, Wilken B and Neubauer F M 2003 Velocity space diffusion and non-gyrotropy of pickup water group ions at comet Grigg-Skjellerup *J. Geophys. Res.* **98** 20,985

[3] Goldstein R *et al* 2015 The Rosetta Ion and Electron Sensor (IES) measurement of the development of pickup ions from comet 67P/Churyumov-Gerasimenko *Geophys. Res. Lett.* 42, 3093-3099

[4] Teolis B D *et al* 2010 Cassini finds an oxygen–carbon dioxide atmosphere at Saturn's icy moon Rhea *Science* **330** 1813-1815

[5] Tokar R L, R E Johnson, M F Thomsen, E C Sittler, A J Coates, R J Wilson, F J Crary, D T Young, G H Jones 2012 Detection of Exospheric O_2^+ at Saturn's Moon Dione *Geophys. Res. Lett.* **39** L03105

[6] Coates A J, Wilken B, Johnstone A D, Jockers K, Glassmeier K-H and Huddleston D E 1990 Bulk properties and velocity distributions of water group ions at comet Halley: Giotto measurements *J.Geophys Res.* **95** 10249-10260

[7] Nilsson H *et al* 2015 Birth of a comet magnetosphere: A spring of water ions *Science* **347** aaa0571

[8] Coates A J, J L Burch, R Goldstein, H Nilsson, G Stenberg Wieser, E Behar and the RPC team 2015 Ion pickup observed at comet 67P with the Rosetta Plasma Consortium (RPC) particle sensors: similarities with previous observations and AMPTE releases, and effects of increasing activity *J. Phys.: Conf. Ser.* **642** 012005

[9] Motchmann U, Glassmeier, K-H 1993 Nongyrotropic distribution of pickup ions at comet P/Grigg-Skjellerup: A possible source of wave activity *J. Geophys. Res.* **98** 20,977-20,983

[10] Brinca, A L, Borda de Agua L, Winske, D 1993 On the stability of nongyrotropic ion populations - A first (analytic and simulation) assessment *J. Geophys. Res.* **98** 7549-7560

[11] Saito Y *et al* 2008 Solar wind proton reflection at the lunar surface: Low energy ion measurement by MAP-PACE onboard SELENE (KAGUYA) *Geophys. Res. Lett.* **35** L24205

[12] Hartle R E *et al*. 2006 Initial Interpretation of Titan Plasma Interaction as Observed by the Cassini Plasma Spectrometer: Comparisons with Voyager 1 *Planet Space Sci.* **54**, 1211-1224

[13] Regoli L H, A J Coates, M F Thomsen, G H Jones, E Roussos, J H Waite, N Krupp and G Cox 2016 Survey of pickup ion signatures in the vicinity of Titan using CAPS/IMS *J. Geophys. Res.* **121** 8317-8328

[14] Coates A J *et al*. 2012 Cassini in Titan's tail: CAPS observations of plasma escape *J. Geophys. Res.* **117**

[15] Coates, A J *et al* 1989 Velocity space diffusion of pick-up ions from the water group at Comet Halley *J. Geophys. Res.* **94** 9983
[16] Coates A J *et al* 1990 Bulk properties and velocity distributions of water group ions at comet Halley: Giotto measurements *J.Geophys Res* **95** 10249
[17] Thomsen M F *et al*. 1987, In-situ observations of a bi-modal ion distribution in the outer coma of Comet Halley, *Astron. Astrophys.* **187** 141
[18] Coates A.J. 1991 Cometary plasma energisation *Ann. Geophys.* **9** 158
[19] Terasawa T and M Scholer 1989 The heliosphere as an astrophysical laboratory for particle acceleration *Science* **244** 1050-1057
[20] McKenna-Lawlor *et al* 1986 Energetic ions in the environment of comet Halley Nature **321** 347
[21] Hynds R J *et al* 1985 Observations of energetic ions from comet Giacobini-Zinner *Scienc*e **232** 361
[22] Gloeckler G *et al* 1986 Cometary pick-up ions observed near Giacobini-Zinner *Geophys. Res. Lett.* **13** 251
[23] Neugebauer M *et al* 1989 The velocity distributions of cometary protons picked up by the solar wind *J. Geophys. Res.* **94** 5227
[24] Tokar R L *et al*. 2008 Cassini detection of water-group pick-up ions in the Enceladus torus Geophys. Res. Lett. **35** L14202
[25] Glassmeier K H 2017 Interaction of the solar wind with comets: a Rosetta perspective *Phil. Trans. R. Soc. A* **375** 20160256
[26] Coates A J et al 1990 Plasma parameters near the comet Halley bow shock *J. Geophys. Res.* **95** 20,701
[27] Coates A J, Mazelle C and Neubauer F M 1997 Bow shock analysis at comets Halley and Grigg Skjellerup *J. Geophys. Res* **102** 7105
[28] Neubauer F M *et al* 1990 Giotto magnetic field observations at the outbound quasi-parallel bow shock of comet Halley *Ann. Geophys.* **8** 463
[29] Johnstone A D *et al* 1986 Ion flow at Halley's comet *Nature* **321** 344
[30] Johnstone A D, Coates A J, Huddleston D E, Jockers K, Wilken B, Borg H, Gurgiolo C, Winningham J D and Amata E 1993 Observations of the solar wind and cometary ions during the encounter between Giotto and comet Grigg-Skjellerup *Astron. Astrophys.* **273** L1-L4
[31] Coates, A J *et al*. 1993 Pickup water group ions at comet Grigg-Skjellerup *Geophys. Res. Lett.* **20** 483-486
[32] McKenna-Lawlor *et al* 1993 Energetic ions at Comet Grigg-Skjellerup measured from the Giotto spacecraft *Nature* **363** 326
[33] Jones, G H *et al*. 2017 Caroline - A search for the source of Earth's water *Adv Space Res.* submitted
[34] Snodgrass, C et al. 2017 The Castalia Mission to Main Belt Comet 133P/Elst-Pizarro *Adv Space Res* submitted